Article

Hydrogeological controls on regional-scale indirect nitrous oxide (N_2O) emission factors for rivers

Richard James Cooper, Sarah Katrina Wexler, Christopher Adams, and Kevin M. Hiscock

Environ. Sci. Technol., **Just Accepted Manuscript** • DOI: 10.1021/acs.est.7b02135 • Publication Date (Web): 25 Aug 2017

Hydrogeological controls on regional-scale indirect nitrous oxide (N_2O) emission factors for rivers

Richard J. Cooper*, Sarah K. Wexler, Christopher A. Adams, Kevin M. Hiscock

School of Environmental Sciences, University of East Anglia, Norwich Research Park, Norwich, NR4 7TJ, UK

*Correspondence: Richard.J.Cooper@uea.ac.uk

Abstract

Indirect nitrous oxide (N_2O) emissions from rivers are currently derived using poorly constrained default IPCC emission factors (EF_{5r}) which yield unreliable flux estimates. Here, we demonstrate how hydrogeological conditions can be used to develop more refined regional-scale EF_{5r} estimates required for compiling accurate national greenhouse gas inventories. Focusing on three UK river catchments with contrasting bedrock and superficial geologies, N_2O and nitrate (NO_3^-) concentrations were analyzed in 651 river water samples collected from 2011 to 2013. Unconfined Cretaceous Chalk bedrock regions yielded the highest median N_2O-N concentration (3.0 μg L^{-1}), EF_{5r} (0.00036) and N_2O-N flux (10.8 kg ha^{-1} a^{-1}). Conversely, regions of bedrock confined by glacial deposits yielded significantly lower median N_2O-N concentration (0.8 μg L^{-1}), EF_{5r} (0.00016) and N_2O-N flux (2.6 kg ha^{-1} a^{-1}), regardless of bedrock type. Bedrock permeability is an important control in regions where groundwater is unconfined, with a high N_2O yield from high permeability Chalk contrasting with significantly lower median N_2O-N concentration (0.7 μg L^{-1}), EF_{5r} (0.00020) and N_2O-N flux (2.0 kg ha^{-1} a^{-1}) on lower permeability unconfined Jurassic mudstone. The evidence presented here demonstrates EF_{5r} can be differentiated by hydrogeological conditions and thus provide a valuable proxy for generating improved regional-scale N_2O emission estimates.

Keywords: Denitrification; streams; climate change; greenhouse gas; IPCC; agriculture

1. Introduction

Nitrous oxide (N_2O) is a powerful greenhouse gas with a global warming potential 265 times greater than carbon dioxide (CO_2) over a 100-year timescale.[1] At a current atmospheric concentration of 329 ppb,[2] N_2O is the third most important well-mixed greenhouse gas behind CO_2 and methane (CH_4), accounting for 6% of total anthropogenic radiative forcing (0.17 W m^{-2}).[1, 3] N_2O is also the single most dominant stratospheric ozone (O_3) depleting substance emitted in the 21st century through its role in the catalytic reduction of O_3 to oxygen (O_2).[1, 4] Importantly, concentrations are estimated to

have increased by 22% since 1750 (270 ppb)[5] and have been growing at an annual rate of 0.75 ppb since the late 1970s.[3]

N_2O is produced as a byproduct of bacterially-driven aerobic nitrification in soils, sediments and waterbodies during the oxidation of ammonium (NH_4^+) to nitrate (NO_3^-), by predominantly autotrophic *Nitrosomonas* and *Nitrobacter* sp.[6-8] N_2O also forms as an obligate intermediate product of denitrification under low oxygen conditions through the bacterial reduction of NO_3^- to nitrogen gas (N_2).[7-9] Furthermore, in oxygen-deficient environments, NH_4^+ can be oxidized to nitrite (NO_2^-) and then reduced to nitric oxide (NO), N_2O and N_2 via nitrifier denitrification.[10]

Current estimates of the total global flux of N_2O into the atmosphere as a result of nitrogen (N) cycling are ~18.8 Tg N a^{-1}, of which ~10.5 Tg N a^{-1} (55%) originate in natural sources.[11] The remaining 45% of emissions are derived from anthropogenic sources (~8.3 Tg N a^{-1}) as a result of perturbations to the N cycle.[11] Agriculture represents the largest anthropogenic source (5.3 – 8.0 Tg N a^{-1}) and can be divided into direct emissions from soils (1.8 – 2.1 Tg N a^{-1}), animal production (2.1 – 2.3 Tg N a^{-1}) and indirect emissions (1.3 – 2.6 Tg N a^{-1}).[11-14] Whilst direct soil emissions have been extensively studied,[6, 15-20] indirect emissions arising from atmospheric deposition (~0.3 – 0.4 Tg N a^{-1}), human sewage (~0.2 – 0.3 Tg N a^{-1}) and N leaching and runoff (~0.6 – 1.9 Tg N a^{-1}) are less well constrained and remain a major source of uncertainty in the global N_2O budget.[21-29]

The Intergovernmental Panel on Climate Change (IPCC) uses emission factors to estimate indirect N_2O emissions from waterbodies arising from N leaching and runoff (EF_5).[13, 30] These are based either on the fraction ($Frac_{LEACH}$) of the original total fertilizer N input into the system that is lost to waterbodies as a result of leaching and runoff from agricultural soils (eq. 1), or simply the ratio of dissolved N_2O to dissolved inorganic nitrogen (DIN) within the waterbody (eq. 2):

$$(1)\ EF_5 = \frac{N_2O\text{–}N}{(total\ N\ input \times Frac_{LEACH})}$$

or

$$(2)\ EF_5 = \frac{N_2O\text{–}N}{NO_3\text{–}N}$$

The IPCC divides EF_5 into three components based on the site of N_2O production in either groundwater (EF_{5g}), rivers (EF_{5r}) or estuaries (EF_{5e}). Since 2006, each component has been assigned a default value of 0.0025 (i.e. 2.5 g of N_2O-N emitted per kg of N in leachate/runoff), thus giving a combined EF_5 of 0.0075.[30] However, these default 'Tier 1' emission factors are poorly constrained due to a paucity of studies, highly uncertain water-air gaseous exchange relationships, and large variability in environmental conditions.[29] Thus, EF_5 has a wide range of uncertainty (0.0005 – 0.025) and has been broadly criticized for either over[14, 31, 32] or under[9, 29] estimating actual N_2O fluxes.

In order to produce more accurate emission estimates, refined 'Tier 3' EF_5 emission factors need to be derived which reflect regional variability in climate, soil type, geology, hydrochemistry, river morphology and land management.[14, 33] In this research, we investigated the impact of hydrogeological conditions upon riverine N_2O emissions as a way of generating improved 'regional-scale' EF_{5r} estimates. Focusing on three UK river catchments with contrasting bedrock (chalk, limestone, sandstone, mudstone, volcanic) and superficial (glacial till, glacial sands/gravels, absent) geologies, we explored whether hydrogeological conditions (high/low permeability, confined/unconfined groundwater) exerted a sufficiently robust control over EF_{5r} that it could be used as a proxy for upscaling N_2O emission estimates that are required for producing national greenhouse gas inventories. We hypothesized such an association could arise due to hydrogeological conditions controlling the infiltration and upwelling of water and dissolved N fertilizers in catchments, which in turn impacts upon the formation and movement of dissolved N_2O gas. It is envisaged the outcomes of this research will provide useful evidence for updating indirect N_2O emission factors used in future IPCC assessment reports.

2. Materials and Methods

2.1 Study Locations

The three river catchments (Avon, Eden and Wensum) and sampling locations investigated in this study were selected to align with the counterpart UK government-funded Demonstration Test Catchments (DTC) program which is evaluating the extent to which on-farm mitigation measures can cost-effectively reduce the impact of agricultural pollution on river ecology.[34]

2.1.1 River Wensum

The River Wensum, Norfolk, is a 78 km length groundwater-dominated lowland (source = 75 m above sea level (a.s.l.)) calcareous river that drains an area of 660 km^2 and has a mean annual discharge of 4.1 m^3 s^{-1} near its outlet[35] (Figure 1; hydrological summaries provided in Figure S1 and Table S1). The catchment is underlain by Cretaceous White Chalk bedrock which is unconfined in the upper catchment and along sections of the river valley where the baseflow index (BFI) is ~0.7–0.9. Over much of the rest of the catchment, the Chalk is confined by superficial deposits of Mid-Pleistocene diamicton glacial tills principally comprising chalky, flint-rich boulder clays of the Sheringham Cliffs (0.2–0.5 m depth) and Lowestoft (0.2–20 m depth) Formations. These are interspersed with layers of glaciofluvial and glaciolacustrine sands and gravels where the BFI is ~0.5–0.7. Within the river valley, Holocene-age alluvium and river terrace deposits are present.[36] Surface soils across the catchment range from low permeability clay loams and sandy peats, to free draining sandy loams. Arable agriculture (wheat, barley, sugar beet, oilseed rape) dominates land use (63%) with the remainder comprising 19% improved grassland, 9% mixed woodland, 5% unimproved

grassland and 4% urban. The mean annual temperature is 10.1°C and the mean annual rainfall total is 674 mm (1981-2010).[37]

2.1.2 River Eden

The River Eden, Cumbria, is a 145 km length surface runoff-dominated upland (source = 675 m a.s.l.) river draining 2288 km^2 with a mean annual discharge of 53.4 m^3 s^{-1} near its outlet.[35] The catchment bedrock comprises a mixture of Permo-Triassic sandstone, lower Palaeozoic igneous formations (Borrowdale Volcanics) and steeply dipping fractured Carboniferous limestone interbedded with sandstone and mudstone units (Figure 1). Quaternary glacial till confines the majority of the bedrock, varying in thickness from 0–30 m across the catchment, whilst alluvium is present in the river valley. The BFI in these confined areas is 0.3–0.5. Soils are mainly sandy clay loam and clay loam; locally deep and well-drained in the headwaters, seasonally wet in the central elevations, moving through to slowly permeable and seasonally waterlogged in lower parts of the catchment. Livestock farming (sheep and dairy) dominates land use, with approximately 50% of land under improved pasture, 20% rough grazing, 16% arable and 8% mixed woodland. The mean annual temperature is 9.4°C and the mean annual precipitation total is 1197 mm (1981-2010).[37]

2.1.3 River Avon

The River Avon, Hampshire, is a 96 km length groundwater-dominated, lowland (source = 120 m a.s.l.) river draining 1717 km^2 with a mean annual discharge of 20.3 m^3 s^{-1} near its outlet.[35] Approximately 85% of the main river flow is supplied by the underlying Cretaceous White Chalk and Upper Greensand bedrock aquifers (BFI = 0.75–0.95). The catchment also contains extensive expanses of low permeability Jurassic Kimmeridge Clay mudstone (BFI = 0.2–0.5). The Chalk and mudstone are largely unconfined across the catchment, but are locally covered by pockets of Quaternary alluvium, head and river terrace deposits. Free-draining, shallow, lime-rich soils overlay the Chalk across much of the catchment, alongside smaller areas of low permeability base-rich clay loam. The catchment has a mixed farming system, with 48% of land under arable cultivation and 32% in grassland for lowland grazing and intensive dairy production. The mean annual temperature is 10.1°C and the mean annual rainfall total is 857 mm (1981-2010).[37]

2.2 Sample Collection

For the River Wensum, samples were collected from 20 sites across the catchment at approximately monthly intervals between February 2011 and May 2013, such that 26 samples were collected from each site and 520 samples were collected in total (Table 1). Of the 20 sites, 16 were tributary streams <10 m width, of which 12 were from sites where the Chalk is confined by glacial deposits (n = 312) and four sites where the Chalk is largely unconfined (n = 104). A further four sites were located on the main channel of the River Wensum (>10 m width) and drained an upstream area encompassing both

131 confined and unconfined Chalk; these samples are henceforth referred to as 'semi-confined' Chalk (*n*
132 = 104). The higher sampling resolution for the River Wensum enabled temporal variability in N_2O
133 dynamics to be assessed for this catchment.

134 For the River Avon, samples were collected from six headwater tributaries on four separate occasions
135 (February, June and October 2012, March 2013). 2-3 replicates were collected from each tributary on
136 each sampling occasion, giving 56 samples in total. Of these, 29 samples came from sites on
137 unconfined Chalk and 27 were on unconfined mudstone.

138 For the River Eden, samples were collected from nine headwater tributaries on four occasions (March,
139 June and October 2012, March 2013). 2–3 replicates were collected from each tributary on each
140 sampling occasion, giving 75 samples in total. Of these, 21 samples were from sites on limestone, 27
141 on sandstone and 27 on volcanics, all confined by glacial deposits.

142 Water samples for dissolved N_2O analysis were collected in 20 mL glass syringes that were flushed
143 three times with river water and any trapped air expelled before the final sample was taken. Samples
144 were returned to cold storage (4°C) within 3 h and analyzed for N_2O within 72 h of collection. Water
145 samples for NO_3^-, NO_2^-, NH_4^+ and dissolved organic carbon (DOC) analysis were grab sampled in 1 L
146 polypropylene bottles and also analyzed within 72 h of collection after filtering. For 240 of the River
147 Wensum grab samples collected between May 2012 and May 2013, an aliquot was filtered through a
148 0.22 μm cellulose acetate filter and frozen at -20^{o}C in preparation for nitrogen and oxygen stable
149 isotope analysis. River water temperatures were measured in-situ with a handheld alcohol
150 thermometer.

151 **2.3 Sample Analysis**

152 Dissolved N_2O concentrations were determined by purge-and-trap gas chromatography with an
153 electron capture detector (Shimadzu GC-ECD) which had a measurement accuracy within ±3% and a
154 detection limit of 0.0008 μg N L^{-1}. Dissolved NO_3^- concentrations were determined by ion
155 chromatography (Dionex ICS-2000) with a precision of ± 0.2 mg N L^{-1}, whilst dissolved NO_2^- and
156 NH_4^+ were determined by a continuous flow analyzer (Skalar SAN++) with precisions of ±1.5 and 5
157 μg L^{-1}, respectively. DOC was determined by a Shimadzu TOC/TN analyzer with a precision of ±0.5
158 mg L^{-1}. Samples for isotopic analysis were prepared using the denitrifier method and analyzed on a
159 GEO 20:20 GC-IRMS with a TG II prep system with a precision of ±0.4‰ for $\delta^{15}N_{NO3}$ and ±0.6‰ for
160 $\delta^{18}O_{NO3}$ (Table S2).

161 **2.4 Fluxes and Emission Factors**

N_2O emission factors for each river water sample were calculated by the mass ratio approach (eq. 2) derived from the measured concentrations of N_2O (mg N L^{-1}) and NO_3^- (mg N L^{-1}). Fluxes of N_2O from the river to the atmosphere where calculated using the water-air gas exchange eq. 3:[38]

$$(3)\quad F = kC_w - \frac{C_a}{k'_h}$$

where F is the flux of N_2O (mol cm^{-2} h^{-1}), subsequently converted into kg N ha^{-1} a^{-1}; k is the gas transfer velocity of N_2O across the water-air interface (cm h^{-1}); C_w is the concentration of N_2O in river water (mol cm^{-3}); C_a is the concentration of N_2O in the atmosphere (mol cm^{-3}); and k'_h is the dimensionless Henry's law constant for N_2O. Estimation of the gas transfer velocity represents a major source of uncertainty in water-atmosphere gas flux calculations and currently no definitive method exists to define k values. [39, 40] The use of benthic turbulence models which incorporate aspects of stream velocity, stream depth, bed roughness and bed slope, likely produce more accurate gas exchange rates for small-to-medium sized rivers such as those studied here.[41] However, with only three of our 35 study sites being gauged (Figure 1), a lack of velocity and depth data meant we instead adopted a wind-based turbulence model where k was calculated as eq. 4:[42]

$$(4)\quad k = 1.91e^{0.35U}\left(\frac{Sc}{600}\right)^{-0.5}$$

where U is the wind speed (m s^{-1}) and Sc is the Schmidt number for N_2O in freshwater adjusted for temperature.[43] Although likely less accurate than a benthic turbulence model, the approach adopted is consistent across all sites and it yields mean k values of 4.0, 4.5 and 4.6 for the Avon, Eden and Wensum catchments, respectively, which are within the range of 3–7 previously recommended.[42] Mean wind speed data (15-min resolution) for the time of sample collection were obtained from local weather stations within each catchment.

The N_2O saturation level (%) was calculated as eq. 5:[28]

$$(5)\quad N_2O_{(sat)} = \frac{N_2O_{(water)}}{N_2O_{(eq)}} \times 100$$

where $N_2O_{(water)}$ is the measured N_2O concentration in river water and $N_2O_{(eq)}$ is the concentration when water is in equilibrium with the atmosphere.[44]

3. Results and Discussion

3.1 Spatial variability

In 99.9% of river water samples, N_2O saturation levels exceeded the atmospheric equilibrium implying almost all sites were acting as a net source of N_2O to the atmosphere. Saturation levels ranged from 90–1305% (median = 283%) for the River Wensum, 116–455% (median = 158%) for the River Eden and 136–17070% (median = 1178%) for the River Avon. Whilst the Wensum and Eden

values are comparable with other studies, saturation levels in the River Avon are towards the upper end of the range previously reported.[14, 26, 45, 46]

Unconfined Chalk regions of the rivers Avon (16.83 μg L^{-1}) and Wensum (2.53 μg L^{-1}) had the highest median N_2O concentrations, contributing to a median concentration for all unconfined Chalk sites of 3.03 μg N L^{-1} (Table 1; Figure 2). Comparatively high median NO_3^- concentrations were also observed for the unconfined Chalk of the Avon (7.01 mg N L^{-1}) and Wensum (9.21 mg N L^{-1}), and together these unconfined Chalk regions yielded the highest median EF_{5r} (0.00036) and N_2O flux (10.8 kg N ha^{-1} a^{-1}). These indirect fluxes are towards the upper end of the range previously reported for rivers draining arable and grassland sites in Europe.[47] However, despite unconfined Chalk regions having the highest EF_{5r} of the different hydrogeological types, the overall median EF_{5r} was 7 times lower than the IPCC default value of 0.0025. Only unconfined Chalk regions of the River Avon had a median EF_{5r} value (0.00235) comparable to the IPCC default.

Regions with confined hydrogeological conditions under glacial deposits yielded the lowest riverine N_2O concentrations, regardless of bedrock type or geographical location. Median N_2O concentrations in river water samples from confined limestone (0.52 μg N L^{-1}), volcanic (0.57 μg N L^{-1}), sandstone (0.61 μg N L^{-1}) and Chalk (0. 79 μg N L^{-1}) bedrock areas were ~4 times lower (*t*-test $p < 0.05$) than recorded in rivers draining areas of unconfined Chalk. The confined Wensum Chalk (5.20 mg N L^{-1}) and confined Eden sandstone (4.52 mg N L^{-1}) also had lower NO_3^- concentrations than the unconfined Wensum Chalk sites, although higher riverine NO_3^- concentrations were recorded on confined limestone (8.61 mg N L^{-1}) in the River Eden. Together, the median EF_{5r} (0.00016) and N_2O flux (2.6 kg ha^{-1} a^{-1}) for all sites confined by glacial deposits were the lowest and second lowest recorded, respectively, with an emission factor 16 times lower than the IPCC default.

The semi-confined Chalk hydrogeological grouping, composed of main River Wensum sites which receive a mix of N_2O and NO_3^- enriched water from unconfined Chalk tributaries and N_2O and NO_3^- depleted water from confined Chalk tributaries, had median N_2O (1.31 μg N L^{-1}) and NO_3^- (5.99 mg N L^{-1}) concentrations, EF_{5r} (0.00022) and flux rate (5.1 kg N ha^{-1} a^{-1}) between that of the confined and unconfined sites. However, in pronounced contrast to the unconfined Chalk sites, streams on unconfined mudstone in the River Avon yielded low median N_2O (0.69 μg N L^{-1}) and NO_3^- (4.46 mg N L^{-1}) concentrations. This indicates that bedrock permeability may exert an important control on N_2O production where it is unconfined, with mudstone permeability being substantially lower than that of Chalk. Emission factors for the unconfined mudstone were highly variable, but median values were ~12 times lower than unconfined Chalk in the same catchment (0.00020), with an emission rate of 2.0 kg ha^{-1} a^{-1}.

Importantly, despite river discharge varying substantially between sampling locations (Figure S1) there is no evidence of a dilution effect in N_2O concentrations at the larger main river sites, nor is

there evidence of a strong N_2O degassing signal as water moves further down the catchment. The hydrogeological conditions at the sampling sites remain the dominant classifier of N_2O concentration and EF_{5r} regardless of discharge or stream order. Evidence for this can be seen in Table 1, where the semi-confined Chalk grouping of the River Wensum is composed solely of the four main river sample locations which have the greatest discharges and highest stream orders. If downstream degassing and dilution were major controls on N_2O, we would expect these semi-confined sites to have lower N_2O concentrations than the other 16 Wensum tributary locations, but this is not the case. Instead, median N_2O concentrations and EF_{5r} values were significantly ($p < 0.05$) higher at the semi-confined main river sites (N_2O = 1.31 μg N L^{-1}; EF_{5r} = 0.00022) than recorded in the confined upstream tributary locations (N_2O = 0.79 μg N L^{-1}; EF_{5r} = 0.00016). Similarly, we also observe that despite having substantially higher discharge (Figure S1), confined tributary sites in the River Eden yield comparable median N_2O concentrations (0.52–0.61 μg N L^{-1}) and EF_{5r} values (0.00007–0.00019) to the confined tributary locations in the River Wensum.

3.2 Temporal variability

Seasonally, riverine N_2O and NO_3^- concentrations were lowest during spring (MAM) and summer (JJA), respectively, regardless of hydrogeological conditions (Table 2). Likewise, the highest NO_3^- concentrations typically occurred across all locations during the winter (DJF), consistent with higher N leaching rates under wetter antecedent conditions. Highest N_2O concentrations did, however, differ by hydrogeological type, being greatest during summer and autumn (SON) in unconfined and semi-confined regions, and during winter in areas of confined Chalk. Emission factors were highest during summer/autumn and lowest during spring, irrespective of hydrogeological type, with these seasonal contrasts being statistically significant (*t*-test $p < 0.05$). Such patterns are broadly consistent with the temporal variability in N_2O concentrations reported previously,[26, 48, 49] and demonstrate that application of a single default EF_{5r} value fails to capture the significant temporal variability in N_2O dynamics and could lead to a misrepresentation of the true N_2O flux. Here, median N_2O flux rates were greatest during winter irrespective of hydrogeological conditions due to significantly higher wind speeds at this time of year yielding a higher gas transfer velocity for the wind disturbance-based Equation 4.

Unconfined Chalk sites consistently had the highest dissolved N_2O concentrations throughout the 28-month period, with concentrations ranging from 0.81–4.70 μg L^{-1} (Figure 3). Conversely, at Chalk sites confined by glacial deposits N_2O concentrations were consistently the lowest and least variable, ranging from 0.32–2.35 μg L^{-1}. The semi-confined Chalk sites were intermediate to the confined and unconfined locations. Peaks in N_2O concentration (e.g. December 2011, June 2012) were associated with rainfall events <24 h before sample collection, which also yielded peaks in the concentration of NO_3^- (Figure S2), NH_4 (Figure S3), NO_2^- (Figure S4) and in EF_{5r} values (Figure S6). Note that the

IPCC typically derives EF_{5r} values based on annual N loads and annual N_2O emissions and thus the instantaneous EF_{5r} values presented in Figure S6 will inherently exhibit greater temporal variability.

3.3 Controls on N_2O dynamics

It is clear from these data that N_2O concentrations, fluxes and emission factors vary between regions of contrasting hydrogeological conditions and it is important to understand why this differentiation occurs in order to confidently upscale EF_{5r} estimates nationally based on this characteristic. We hypothesize that in all three catchments, fertilizer inputs are hydrolyzed to NH_4^+ and readily nitrified to NO_3^- in the soil with further nitrification occurring in stream. In unconfined Chalk regions, NO_3^- and N_2O from the soil are rapidly transported in infiltrating water down to the well-mixed groundwater zone in the high permeability Chalk. As N_2O and NO_3^- enriched groundwater comprises the major proportion of river flow in these regions (BFI = 0.70–0.95), high N_2O and NO_3^- concentrations are subsequently observed instream, alongside elevated EF_{5r} values. Conversely, in regions of confined groundwater and smaller BFI (0.40–0.70), lower permeability glacial deposits reduce infiltration rates and allow low oxygen conditions to develop where denitrification and/or nitrifer denitrification can occur before the infiltrating water recharges groundwater. This process partially protects groundwater from NO_3^- leaching and results in lower NO_3^- and N_2O concentrations at these sites.[50] Although regions of unconfined mudstone are not protected by overlying glacial deposits, the lower permeability of the mudstone relative to the Chalk results in similar opportunities for denitrification and/or nitrifier denitrification, thus resulting in lower NO_3^- concentrations, reduced rates of soil-to-river N_2O transfer and lower EF_{5r} values. This hypothesis is supported by the stable isotope data (Figure 4b).

The nitrogen ($\delta^{15}N$) and oxygen ($\delta^{18}O$) isotopic composition of NO_3^- can be used to infer mixing of sources of NO_3^- with differing isotopic composition and to indicate the dominance of nitrification and denitrification (see Supporting Information). The fractionation ratio of $\delta^{15}N_{NO3}$ to $\delta^{18}O_{NO3}$ for the Wensum samples is 0.41 (Figure 4b), providing some evidence of denitrification across the catchment drainage network. Mixing of atmospheric and fertilizer direct NO_3^- sources with partially denitrified NO_3^- raises the bulk $\delta^{18}O_{NO3}$ and produces scatter above the denitrification slope (Figure 4b). Variation in pre-nitrification $\delta^{15}N_{NH4}$ is reflected in post-nitrification $\delta^{15}N_{NO3}$, producing scatter on the $\delta^{15}N_{NO3}$ axis. Together these mixing effects result in a weak relationship between $\delta^{18}O_{NO3}$ and $\delta^{15}N_{NO3}$ ($R^2 = 0.375$), reflecting the combined effects of mixing and denitrification.

The heaviest expected $\delta^{18}O_{NO3}$ produced from nitrification of NH_4^+ in the Wensum catchment is 3.8‰.[51] This value is derived from the incorporation of oxygen from ambient water and air during nitrification at an initial ratio of 2:1,[52, 53] as well as from measurements of $\delta^{18}O_{H2O}$ in rivers, tributaries, field drains, streambed piezometers and boreholes in the Wensum catchment ($\delta^{18}O_{H2O}$ = 6.0‰ to -7.5‰).[50] This upper limit would not be affected by any abiotic oxygen exchange between

300 NO_2^- and H_2O,[54] because this would result in isotopically lighter $\delta^{18}O_{NO3}$. Fertilizer and precipitation
301 direct sources of NO_3^- ($\delta^{18}O_{NO3}$ >20‰) have $\delta^{18}O_{NO3}$ values clearly differentiated from that of NO_3^-
302 produced from nitrification in the Wensum catchment, thus $\delta^{18}O_{NO3} \leq 3.8$‰ can be used as an
303 indicator of NO_3^- from nitrification (Figure 4b).

304 There is a positive relationship between the relative dominance of nitrification NO_3^- and median N_2O
305 concentrations with hydrogeological setting. The highest proportion of samples containing
306 nitrification NO_3^- ($\delta^{18}O_{NO3} \leq 3.8$‰) were from unconfined Chalk sites (42% of 48 samples). These
307 sites also produced the highest median N_2O concentrations (2.53 μg N_2O L^{-1}). In comparison, the
308 confined Chalk produced the lowest proportion of samples containing nitrification NO_3^- (7% of 132
309 samples), with the lowest median N_2O concentrations (0.79 μg N_2O L^{-1}). The proportion of
310 nitrification NO_3^- from semi-confined sites was between that of unconfined and confined Chalk sites
311 (22% of 60 samples) with a median N_2O concentration of 1.31 μg N_2O L^{-1}. This relationship indicates
312 that nitrification, rather than denitrification, is the dominant N_2O production process in the Wensum
313 catchment. We suggest that in unconfined Chalk sites, infiltration of recharge water occurs rapidly to
314 well-mixed shallow groundwater. Baseflow transports dissolved nitrification NO_3^-, by-product N_2O
315 and denitrification-inhibiting dissolved oxygen (DO saturation = 89–97%[50]) into the river.
316 Denitrification may also be inhibited in the unconfined sites by a relatively low availability of labile
317 carbon, with a mean DOC:NO_3^- ratio <1 at unconfined Chalk sites and >1 at confined sites.

318 Across all hydrogeological types in the Wensum catchment, N_2O concentrations and saturation levels
319 were only weakly correlated with pH (R^2 = <0.08) and water temperature (R^2 = < 0.07), indicating
320 these variables were not directly acting as abiotic controls on N_2O production (Figure S9). Stronger
321 negative correlations were, however, established between EF_{5r} and total N (R^2 = 0.35–0.59) providing
322 evidence of decreasing (de)nitrification efficiency with increasing N inputs due to progressive
323 biological saturation.[31] Low NH_4^+ concentrations at unconfined Chalk sites indicate nitrification is
324 acting as a sink for NH_4^+ (Figure S9).

325 **3.4 Implications and recommendations**

326 The evidence presented here clearly demonstrates that N_2O emission factors vary significantly
327 between regions of contrasting hydrogeological type. Given the inherent regional nature of
328 hydrogeological variability as determined by the distribution of bedrock and superficial geologies, this
329 robust association with EF_{5r} values indicates that hydrogeological conditions could be used as a
330 defining environmental characteristic for upscaling N_2O emission estimates. Undoubtedly there is a
331 need to further explore whether this association is maintained across a wider range of hydrogeological
332 settings than those investigated here. Nevertheless, regional variability in hydrogeological conditions
333 could be used to generate improved regional-scale EF_{5r} estimates that are essential for developing
334 more accurate national greenhouse gas inventories. Such an approach would address the pressing need

to produce more refined EF_5 values than the current broad-brush method adopted by the IPCC; a call which has been repeatedly emphasized in numerous studies over the past decade.[14, 26, 32, 38] The unsuitable nature of the default IPCC EF_{5r} value is again highlighted here with 98% of samples having an EF_{5r} lower than the default 0.0025 value, this despite the downward revision of EF_{5r} during the 2006 IPCC Fourth Assessment Report.[30] We therefore encourage researchers to investigate if the association between hydrogeology and EF_{5r} is maintained across contrasting river basins. If it is, it should be possible to calibrate hydrogeological-specific EF_{5r} emission factors which can be overlain onto existing global spatial lithological[55, 56] and hydrological[57] databases as a means of effectively upscaling indirect N_2O emissions from rivers draining defined hydrogeological regions.

Supporting Information

The Supporting Information contains hydrological summaries for the study locations (Figure S1; Table S1); description of the laboratory procedures; water quality time-series for the River Wensum (Figures S2–S7); extended discussion of the stable isotope data (Figure S8; Table S2); and regression plots for nitrogen species (Figure S9). The project data are provided in Excel spreadsheet format.

Author Information

*Corresponding Author: Richard J. Cooper; Richard.J.Cooper@uea.ac.uk; +44(0)1603592922;
School of Environmental Sciences, University of East Anglia, Norwich Research Park, Norwich NR4 7TJ, UK

Acknowledgements

This research was funded by Defra under the UK Inventory of Agricultural Greenhouse Gas Emissions Platform (AC0116). We are grateful to the Avon and Eden Demonstration Test Catchments for providing logistical support and to Lee Gumm for assistance with data analysis.

References

1. Myhre, G.; Shindell, D.; Bréon, F.-M.; Collins, W.; Fuglestvedt, J.; J., H.; Koch, D.; Lamarque, J.-F.; Lee, D.; Mendoza, B.; Nakajima, T.; Robock, A.; Stephens, G.; Takemura, T.; Zhang, H., Anthropogenic and Natural Radiative Forcing. In *Climate Change 2013: The Physical Science Basis. Contribution of Working Group I to the Fifth Assessment Report of the Intergovernmental Panel on Climate Change.*, Stocker, T. F.; Qin, D.; Plattner, G.-K.; Tignor, M.; Allen, S. K.; Boschung, J.; Nauels, A.; Xia, Y.; V., B.; Midgley, P. M., Eds. Cambridge University Press, Cambridge, United Kingdom: 2013.
2. NOAA Earth System Research Laboratory. https://www.esrl.noaa.gov/gmd/dv/data/?parameter_name=Nitrous%2BOxide (03/03/2017),
3. Hartmann, D. L.; Klein Tank, A. M. G.; Rusticucci, M.; Alexander, L. V.; Brönnimann, S.; Charabi, Y.; Dentener, F. J.; Dlugokencky, E. J.; Easterling, D. R.; Kaplan, A.; Soden, B. J.; Thorne, P. W.; Wild, M.; Zhai, P. M., Observations: Atmosphere and Surface. In *Climate Change 2013: The Physical Science Basis. Contribution of Working Group I to the Fifth Assessment Report of the Intergovernmental Panel on Climate Change*, Stocker, T. F.; Qin, D.; Plattner, G.-K.; Tignor, M.;

Allen, S. K.; Boschung, J.; Nauels, A.; Xia, Y.; Bex, V.; Midgley, P. M., Eds. Cambridge University Press, Cambridge, United Kingdom: 2013.
4. Ravishankara, A. R.; Daniel, J. S.; Portmann, R. W., Nitrous oxide (N_2O): the dominant ozone-depleting substance emitted in the 21st century. *Science* **2009,** *326*, 123-125.
5. Davidson, E. A., The contribution of manure and fertilizer nitrogen to atmospheric nitrous oxide since 1860. *Nature Geoscience* **2009,** *2*, (9), 659-662.
6. Bremner, J. M.; Blackmer, A. M., Nitrous oxide: emission from soils during nitrification of fertilizer nitrogen. *Science* **1978,** *199*, (4326), 295-296.
7. Strauss, E. A.; Richardson, W. B.; Bartsch, L. A.; Cavanaugh, J. C.; Bruesewitz, D. A.; Imker, H.; Heinz, J. A.; Soballe, D. M., Nitrification in the Upper Mississippi River: patterns, controls, and contribution to the NO_3 budget. *Journal of the North American Benthological Society* **2004,** *23*, (1), 1-14.
8. Mulholland, P. J.; Helton, A. M.; Poole, G. C.; Hall, R. O.; Hamilton, S. K.; Peterson, B. J.; Tank, J. L.; Ashkenas, L. R.; Cooper, L. W.; Dahm, C. N.; Dodds, W. K.; Findlay, S. E.; Gregory, S. V.; Grimm, N. B.; Johnson, S. L.; McDowell, W. H.; Meyer, J. L.; Valett, H. M.; Webster, J. R.; Arango, C. P.; Beaulieu, J. J.; Bernot, M. J.; Burgin, A. J.; Crenshaw, C. L.; Johnson, L. T.; Niederlehner, B. R.; O'Brien, J. M.; Potter, J. D.; Sheibley, R. W.; Sobota, D. J.; Thomas, S. M., Stream denitrification across biomes and its response to anthropogenic nitrate loading. *Nature* **2008,** *452*, (7184), 202-205.
9. Beaulieu, J. J.; Tank, J. L.; Hamilton, S. K.; Wollheim, W. M.; Hall, R. O.; Mulholland, P. J.; Peterson, B. J.; Ashkenas, L. R.; Cooper, L. W.; Dahm, C. N.; Dodds, W. K.; Grimm, N. B.; Johnson, S. L.; McDowell, W. H.; Poole, G. C.; Maurice Valett, H.; Arango, C. P.; Bernot, M. J.; Burgin, A. J.; Crenshaw, C. L.; Helton, A. M.; Johnson, L. T.; O'Brien, J. M.; Potter, J. D.; Sheibley, R. W.; Sobota, D. J.; Thomas, S. M., Nitrous oxide emission from denitrification in stream and river networks. *PNAS* **2011,** *108*, (1), 214-219.
10. Kool, D. M.; Dolfing, J.; Wrage, N.; Van Groenigen, J. W., Nitrifier denitrification as a distinct and significant source of nitrous oxide from soil. *Soil Biology and Biochemistry* **2011,** *43*, (1), 174-178.
11. Syakila, A.; Kroeze, C., The global nitrous oxide budget revisited. *Greenhouse Gas Measurement and Management* **2011,** *1*, (1), 17-26.
12. Mosier, A.; Kroeze, C.; Nevison, C.; Oenema, O.; Seitzinger, S.; van Cleemput, O., Closing the global N2O budget: nitrous oxide emissions through the agricultural nitrogen cycle. *Nutrient Cycling in Agroecosystems* **1998,** *52*, 225-248.
13. Nevison, C., Review of the IPCC methodology for estimating nitrous oxide emissions associated with agricultural leaching and runoff. *Chemosphere* **2000,** *2*, 493-500.
14. Clough, T. J.; Buckthought, L. E.; Kelliher, F. M.; Sherlock, R. R., Diurnal fluctuations of dissolved nitrous oxide (N2O) concentrations and estimates of N2O emissions from a spring-fed river: implications for IPCC methodology. *Global Change Biology* **2007,** *13*, (5), 1016-1027.
15. Bouwman, A. F., Direct emission of nitrous oxide from agricultural soils. *Nutrient Cycling in Agroecosystems* **1996,** *46*, 53-70.
16. Davidson, E. A.; Kingerlee, W., A global inventory of nitric oxide emissions from soils. *Nutrient Cycling in Agroecosystems* **1997,** *48*, 14.
17. Lesschen, J. P.; Velthof, G. L.; de Vries, W.; Kros, J., Differentiation of nitrous oxide emission factors for agricultural soils. *Environ Pollut* **2011,** *159*, (11), 3215-22.
18. Smith, K. A.; Dobbie, K. E.; Thorman, R.; Watson, C. J.; Chadwick, D. R.; Yamulki, S.; Ball, B. C., The effect of N fertilizer forms on nitrous oxide emissions from UK arable land and grassland. *Nutrient Cycling in Agroecosystems* **2012,** *93*, 127-149.
19. Butterbach-Bahl, K.; Baggs, E. M.; Dannenmann, M.; Kiese, R.; Zechmeister-Boltenstern, S., Nitrous oxide emissions from soils: how well do we understand the processes and their controls? *Philos Trans R Soc Lond B Biol Sci* **2013,** *368*, (1621), 20130122.
20. Griffis, T. J.; Lee, X.; Baker, J. M.; Russelle, M. P.; Zhang, X.; Venterea, R.; Millet, D. B., Reconciling the differences between top-down and bottom-up estimates of nitrous oxide emissions for the U.S. Corn Belt. *Global Biogeochemical Cycles* **2013,** *27*, (3), 746-754.
21. Reay, D. S.; Davidson, E. A.; Smith, K. A.; Smith, P.; Melillo, J. M.; Dentener, F.; Crutzen, P. J., Global agriculture and nitrous oxide emissions. *Nature Climate Change* **2012,** *2*, (6), 410-416.

22. Reay, D. S.; Smith, K. A.; Edwards, A. C., Nitrous oxide emission from agricultural drainage waters. *Global Change Biology* **2003,** *9*, 195-203.
23. Reay, D. S.; Smith, K. A.; Edwards, A. C.; Hiscock, K. M.; Dong, L. F.; Nedwell, D. B., Indirect nitrous oxide emissions: Revised emission factors. *Environmental Sciences* **2005,** *2*, (2-3), 153-158.
24. Well, R.; Weymann, D.; Flessa, H., Recent research progress on the significance of aquatic systems for indirect agricultural N2O emissions. *Environmental Sciences* **2005,** *2*, (2-3), 143-151.
25. Beaulieu, J. J.; Arango, C. P.; Hamilton, S. K.; Tank, J. L., The production and emission of nitrous oxide from headwater streams in the Midwestern United States. *Global Change Biology* **2008,** *14*, (4), 878-894.
26. Hinshaw, S. E.; Dahlgren, R. A., Dissolved nitrous oxide concentrations and fluxes from the eutrophic San Joaquin River, California. *Environ Sci Technol* **2013,** *47*, (3), 1313-1322.
27. Yu, Z.; Deng, H.; Wang, D.; Ye, M.; Tan, Y.; Li, Y.; Chen, Z.; Xu, S., Nitrous oxide emissions in the Shanghai river network: implications for the effects of urban sewage and IPCC methodology. *Glob Chang Biol* **2013,** *19*, (10), 2999-3010.
28. Chen, N.; Wu, J.; Zhou, X.; Chen, Z.; Lu, T., Riverine N2O production, emissions and export from a region dominated by agriculture in Southeast Asia (Jiulong River). *Agriculture, Ecosystems & Environment* **2015,** *208*, 37-47.
29. Turner, P. A.; Griffis, T. J.; Lee, X.; Baker, J. M.; Venterea, R. T.; Wood, J. D., Indirect nitrous oxide emissions from streams within the US Corn Belt scale with stream order. *Proc Natl Acad Sci U S A* **2015,** *112*, (32), 9839-9843.
30. De Klein, C.; Novoa, R. S. A.; Ogle, S.; Smith, K. A.; Rochette, P.; Wirth, T. C., N_2O emissions from managed soils, and CO_2 emissions from lime and urea application. In *2006 IPCC guidelines for national greenhouse gas inventories*, Cambridge University Press, Cambridge, United Kingdom: 2006; p 54.
31. Hu, M.; Chen, D.; Dahlgren, R. A., Modeling nitrous oxide emission from rivers: a global assessment. *Glob Chang Biol* **2016,** *22*, (11), 3566-3582.
32. Hama-Aziz, Z. Q.; Hiscock, K. M.; Cooper, R. J., Indirect Nitrous Oxide Emission Factors for Agricultural Field Drains and Headwater Streams. *Environ Sci Technol* **2017,** *51*, (1), 7.
33. Skiba, U.; Jones, S. K.; Dragosits, U.; Drewer, J.; Fowler, D.; Rees, R. M.; Pappa, V. A.; Cardenas, L.; Chadwick, D.; Yamulki, S.; Manning, A. J., UK emissions of the greenhouse gas nitrous oxide. *Philos Trans R Soc Lond B Biol Sci* **2012,** *367*, (1593), 1175-1185.
34. McGonigle, D. F.; Burke, S. P.; Collins, A. L.; Gartner, R.; Haft, M. R.; Harris, R. C.; Haygarth, P. M.; Hedges, M. C.; Hiscock, K. M.; Lovett, A. A., Developing Demonstration Test Catchments as a platform for transdisciplinary land management research in England and Wales. *Environ Sci Process Impacts* **2014,** *16*, (7), 1618-1628.
35. CEH National River Flow Archive. https://nrfa.ceh.ac.uk/data/search (17/07/2017),
36. Hiscock, K. M.; Dennis, P. F.; Saynor, P. R.; Thomas, M. O., Hydrochemical and stable isotope evidence for the extent and nature of the effective Chalk aquifer of north Norfolk, UK. *Journal of Hydrology* **1996,** *180*, 29.
37. Meteorological-Office UK Climate Averages. http://www.metoffice.gov.uk/public/weather/climate/?tab=climateStations (17/07/2017),
38. Outram, F. N.; Hiscock, K. M., Indirect nitrous oxide emissions from surface water bodies in a lowland arable catchment: a significant contribution to agricultural greenhouse gas budgets? *Environ Sci Technol* **2012,** *46*, (15), 8156-8163.
39. Beaulieu, J. J.; Shuster, W. D.; Rebholz, J. A., Controls on gas transfer velocities in a large river. *Journal of Geophysical Research: Biogeosciences* **2012,** *117*, (G2).
40. Raymond, P. A.; Zappa, C. J.; Butman, D.; Bott, T. L.; Potter, J.; Mulholland, P.; Laursen, A. E.; McDowell, W. H.; Newbold, D., Scaling the gas transfer velocity and hydraulic geometry in streams and small rivers. *Limnology and Oceanography: Fluids and Environments* **2012,** *2*, (1), 41-53.
41. Baulch, H. M.; Venkiteswaran, J. J.; Dillon, P. J.; Maranger, R., Revisiting the application of open-channel estimates of denitrification. *Limnology and Oceanography: Methods* **2010,** *8*, (5), 202-215.

42. Raymond, P. A.; Cole, J., Gas exchange in rivers and estuaries: choosing a gas transfer velocity. *Estuaries* **2001,** *24*, (2), 312-317.
43. Wanninkhof, R., Relationship between wind speed and gas exchange over the ocean. *Journal of Geophysical Research* **1992,** *97*, (C5), 7373-7382.
44. Weiss, R. F.; Price, B. A., Nitrous oxide solubility in water and seawater. *Marine Chemistry* **1980,** *8*, 13.
45. Cole, J.; Caraco, N., Emissions of nitrous oxide (N_2O) from a tidal, freshwater river, the Hudson River, New York. *Environmental Science & Technology* **2001,** *35*, (6), 6.
46. Xia, Y.; Li, Y.; Li, X.; Guo, M.; She, D.; Yan, X., Diurnal pattern in nitrous oxide emissions from a sewage-enriched river. *Chemosphere* **2013,** *92*, (4), 421-428.
47. Garnier, J.; Billen, G.; Vilain, G.; Martinez, A.; Silvestre, M.; Mounier, E.; Toche, F., Nitrous oxide (N_2O) in the Seine river and basin: Observations and budgets. *Agriculture, Ecosystems & Environment* **2009,** *133*, (3-4), 223-233.
48. Wilcock, R. J.; Sorrell, B. K., Emissions of Greenhouse Gases CH4 and N2O from Low-gradient Streams in Agriculturally Developed Catchments. *Water, Air, and Soil Pollution* **2008,** *188*, (1-4), 155-170.
49. Hama-Aziz, Z. Q.; Hiscock, K. M.; Cooper, R. J., Dissolved nitrous oxide (N_2O) dynamics in agricultural field drains and headwater streams in an intensive arable catchment. *Hydrological Processes* **2017,** *31*, (6), 1371-1381.
50. Wexler, S. K. An investigation into the sources, cycling and attenuation of nitrate in an agricultural lowland catchment using stable isotopes of nitrogen and oxygen in nitrate. University of East Anglia, 2011.
51. Wexler, S. K.; Hiscock, K. M.; Dennis, P. F., Catchment-scale quantification of hyporheic denitrification using an isotopic and solute flux approach. *Environ Sci Technol* **2011,** *45*, (9), 3967-3973.
52. Andersson, K. K.; Hooper, A. B., O_2 and H_2O are each the source of one O in NO^{-2} produced from NH_3 by Nitrosomonas: ^{15}N-NMR evidence. *FEBS Letters* **1983,** *164*, (2), 236-240.
53. Kumar, S.; Nicholas, D. J. D.; Williams, E. H., Definitive ^{15}N NMR evidence that water serves as a source of 'O' during nitrite oxidation by Nitrobacter agilis. *FEBS Letters* **1983,** *152*, (1), 71-74.
54. Snider, D. M.; Spoelstra, J.; Schiff, S. L.; Venkiteswaran, J. J., Stable oxygen isotope ratios of nitrate produced from nitrification: ^{18}O-labeled water incubations of agricultural and temperate forest soils. *Environmental Science & Technology* **2010,** *44*, 5358-5364.
55. Gleeson, T.; Smith, L.; Moosdorf, N.; Hartmann, J.; Dürr, H. H.; Manning, A. H.; van Beek, L. P. H.; Jellinek, A. M., Mapping permeability over the surface of the Earth. *Geophysical Research Letters* **2011,** *38*, (2), L02401.
56. Dürr, H. H.; Meybeck, M.; Dürr, S. H., Lithologic composition of the Earth's continental surfaces derived from a new digital map emphasizing riverine material transfer. *Global Biogeochemical Cycles* **2005,** *19*, (4), GB4S10.
57. Doll, P.; Fiedler, K., Global-scale modeling of groundwater recharge. *Hydrology and Earth System Sciences* **2008,** *12*, 863-885.

Figure Captions

Figure 1: Location of the three UK study catchments with associated bedrock and superficial geologies. Based upon DiGMapGB-625, with the permission of the British Geological Survey.

Figure 2: Violin plot summaries of (a) dissolved nitrous oxide concentration, (b) nitrate concentration, (c) EF_{5r} emission factor and (d) nitrous oxide flux for all river water samples by hydrogeological type. Various includes limestone, chalk, sandstone and volcanic bedrock.

Figure 3: Time-series of dissolved nitrous oxide concentrations in the River Wensum catchment between February 2011 and May 2013.

Figure 4: (a) Dissolved nitrous oxide and nitrate concentrations for all catchments grouped by hydrogeological type. Various includes limestone, chalk, sandstone and volcanic bedrock. Lines are linear regressions; (b) Stable isotope composition of nitrogen and oxygen in nitrate for River Wensum samples collected between May 2012 and May 2013. Diagonal line represents the denitrification isotope effect (regression line for all data; R^2=0.375). Dark grey area delineates expected range of isotopic composition from 'nitrification' nitrate in the Wensum catchment. Vertical and horizontal arrows denote expected ranges of labelled processes.

Tables

Table 1: Summary river water data for different catchments and contrasting hydrogeological types. Values presented as medians with one standard deviation in parentheses. Different superscript letters denote significant differences (*t*-test $p < 0.05$) between hydrogeological types within each catchment.

Catchment	Bedrock	Hydrogeological type	*N* samples	N_2O (µg N L^{-1})	NO_3^- (mg N L^{-1})	Emission Factor (EF_{5r})	Indirect N_2O flux (kg N ha^{-1} a^{-1})
Wensum	Chalk	Unconfined	104	2.53 (0.92)^{a}	9.21 (2.02)^{a}	0.00030 (0.00015)^{a}	9.75 (4.57)^{a}
	Chalk	Semi-confined	104	1.31 (0.40)^{b}	5.99 (1.81)^{b}	0.00022 (0.00008)^{b}	5.09 (2.03)^{b}
	Chalk	Confined; glacial deposits	312	0.79 (0.26)^{c}	5.20 (2.24)^{c}	0.00016 (0.00014)^{c}	2.72 (1.62)^{c}
Eden	Limestone	Confined; glacial deposits	21	0.52 (0.09)^{a}	8.61 (1.33)^{a}	0.00007 (0.00001)^{a}	1.50 (0.64)^{a}
	Volcanics	Confined; glacial deposits	27	0.57 (0.34)^{a}	-	-	1.72 (1.10)^{b}
	Sandstone	Confined; glacial deposits	27	0.61 (0.44)^{b}	4.52 (5.21)^{a}	0.00019 (0.00010)^{b}	2.19 (1.84)^{b}
Avon	Chalk	Unconfined	29	16.83 (12.93)^{a}	7.01 (0.41)^{a}	0.00235 (0.00186)^{a}	60.14 (51.98)^{a}
	Mudstone	Unconfined	27	0.69 (0.95)^{b}	4.46 (2.49)^{b}	0.00020 (0.00057)^{b}	1.95 (8.98)^{b}
All	Chalk	Unconfined	133	3.03 (9.14)^{a}	8.51 (2.02)^{a}	0.00036 (0.00134)^{a}	10.83 (33.70)^{a}
	Chalk	Semi-confined	104	1.31 (0.40)^{b}	5.99 (1.81)^{c}	0.00022 (0.00008)^{b}	5.09 (2.03)^{b}
	Mudstone	Unconfined	27	0.69 (0.95)^{bc}	4.46 (2.49)^{b}	0.00020 (0.00056)^{a}	1.95 (8.98)^{bc}
	Various*	Confined; glacial deposits	387	0.76 (0.28)^{c}	5.26 (2.65)^{d}	0.00016 (0.00014)^{c}	2.58 (4.62)^{c}

* includes limestone, chalk, sandstone and volcanic bedrock

Table 2: Seasonal variability in nitrogen dynamics for sites with contrasting hydrogeological types in the River Wensum catchment. Values presented as medians with one standard deviation in parentheses. Different superscript letters denote significant differences (*t*-test $p < 0.05$) between seasons with the same hydrogeological type.

Hydrogeological type	N samples	Parameter	Spring (MAM)	Summer (JJA)	Autumn (SON)	Winter (DJF)
Unconfined Chalk	104	N_2O (µg N L^{-1})	2.07 (0.90)^{a}	3.06 (0.83)^{b}	3.21 (0.93)^{b}	2.47 (0.81)^{ab}
		NO_3^- (mg N L^{-1})	9.70 (1.44)^{a}	8.22 (1.10)^{b}	8.72 (2.64)^{ab}	10.00 (2.12)^{a}
		EF_{5r}	0.00021 (0.00010)^{a}	0.00039 (0.00011)^{b}	0.00039 (0.00020)^{b}	0.00027 (0.00009)^{a}
		Flux (kg N ha^{-1} a^{-1})	8.14(5.11)^{ab}	9.06 (2.90)^{b}	10.40 (3.84)^{ab}	11.82 (5.15)^{a}
Semi-confined Chalk	104	N_2O (µg N L^{-1})	1.10 (0.36)^{a}	1.42 (0.37)^{b}	1.39 (0.45)^{b}	1.26 (0.38)^{ab}
		NO_3^- (mg N L^{-1})	6.68 (1.90)^{a}	4.60 (1.62)^{b}	5.90 (1.41)^{a}	6.71 (1.84)^{a}
		EF_{5r}	0.00019 (0.00005)^{a}	0.00030 (0.00009)^{b}	0.00025 (0.00005)^{c}	0.00020 (0.00006)^{a}
		Flux (kg N ha^{-1} a^{-1})	5.21 (2.07)^{a}	4.19 (1.61)^{b}	4.31 (1.99)^{ab}	5.89 (2.00)^{c}
Confined Chalk	312	N_2O (µg N L^{-1})	0.75 (0.24)^{a}	0.74 (0.26)^{a}	0.79 (0.24)^{a}	0.87 (0.29)^{b}
		NO_3^- (mg N L^{-1})	5.81 (1.90)^{a}	4.31 (2.27)^{b}	4.72 (2.39)^{b}	5.59 (2.21)^{a}
		EF_{5r}	0.00015 (0.00006)^{a}	0.00019 (0.00024)^{b}	0.00016 (0.00013)^{bc}	0.00016 (0.00008)^{c}
		Flux (kg N ha^{-1} a^{-1})	2.81 (1.46)^{a}	2.01 (1.02)^{b}	2.48 (0.89)^{c}	3.94 (1.93)^{d}

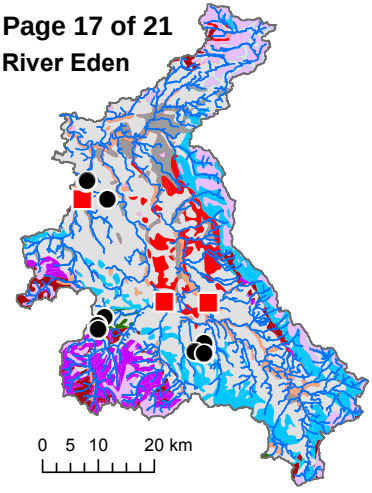

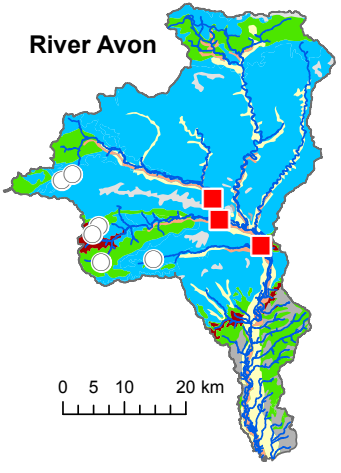

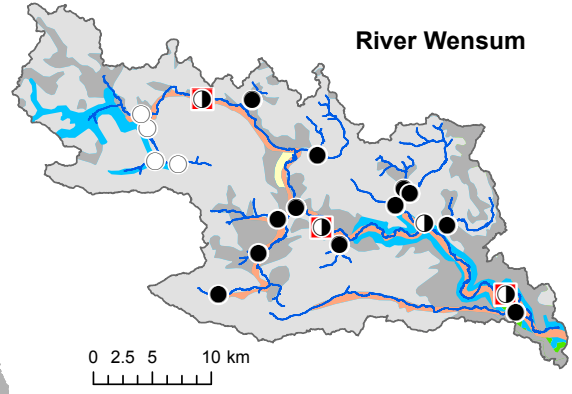

Sampling Location Hydrogeology

- Unconfined
- Semi-confined
- Confined
- Gauging station

Superficial Geology

- Sand and gravel
- Diamicton till
- River terrace deposits
- Alluvium
- Peat

Bedrock Geology

- Limestone/Chalk
- Mixed sedimentary
- Sandstone
- Mudstone
- Volcanics
- Conglomerate

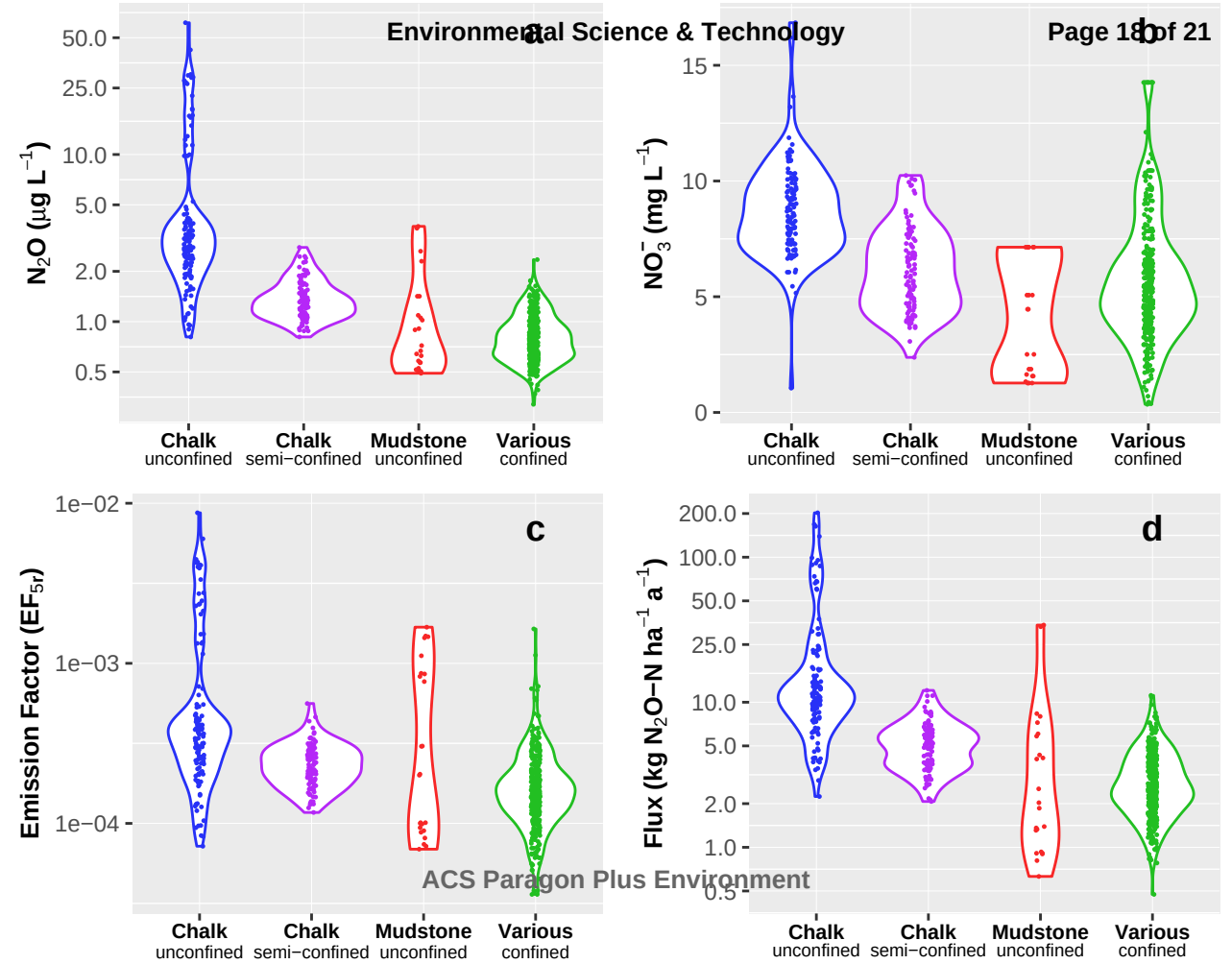

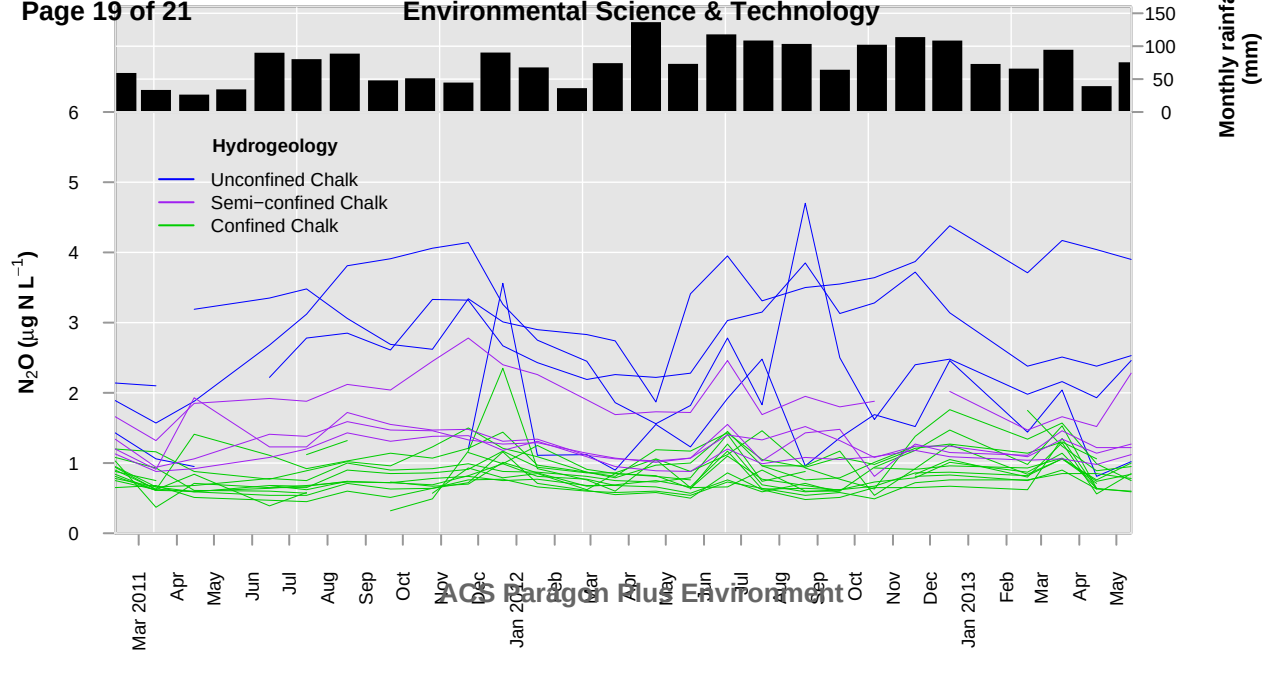

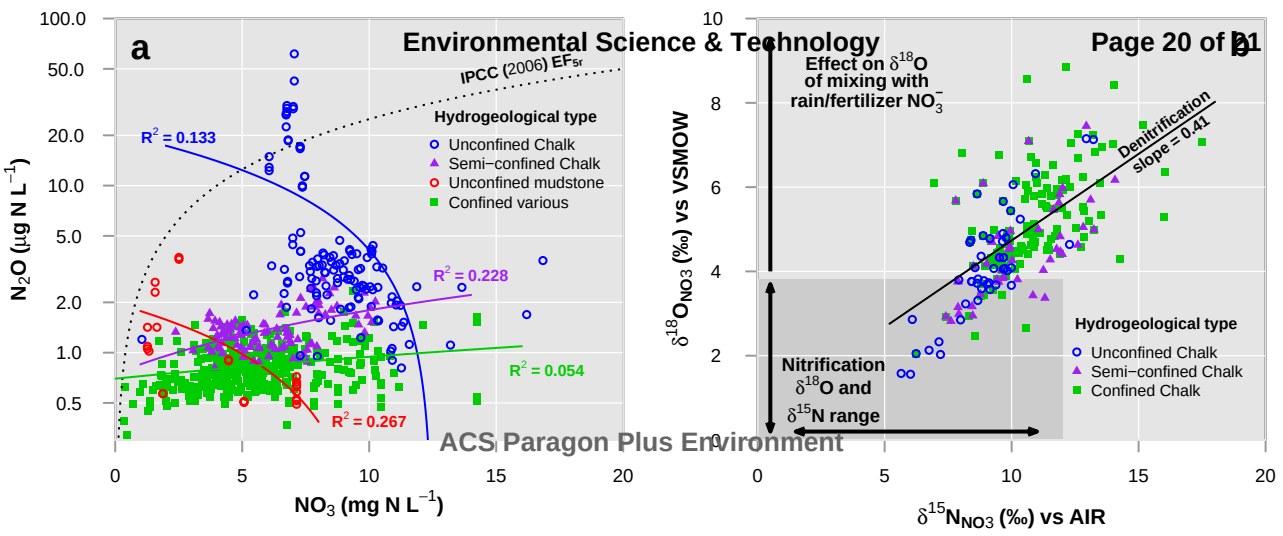

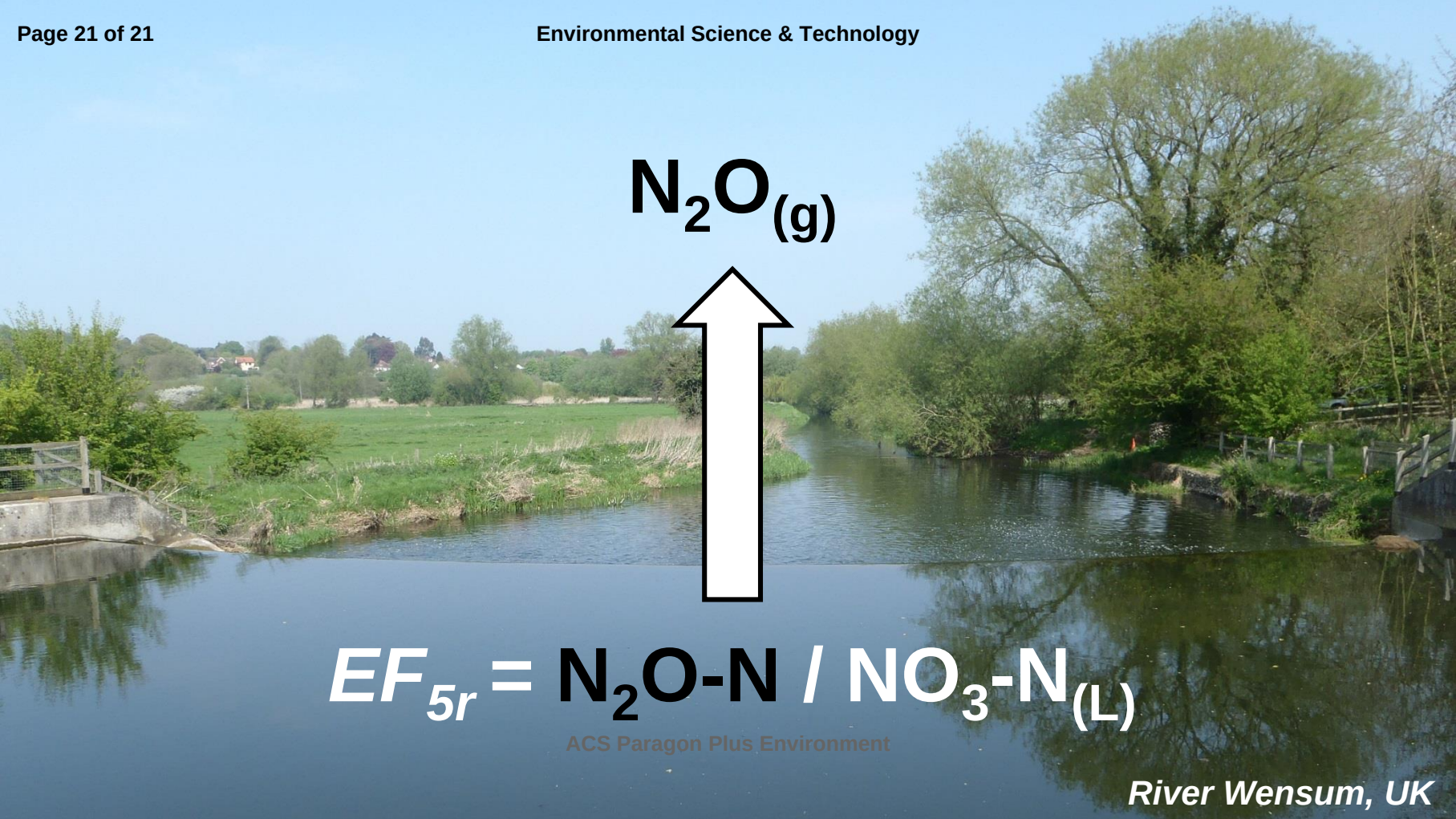
$N_2O_{(g)}$
$EF_{5r} = N_2O\text{-}N / NO_3\text{-}N_{(L)}$
ACS Paragon Plus Environment
River Wensum, UK